THE JOURNAL OF PHYSICAL CHEMISTRY C

Article

pubs.acs.org/JPCC

Quantum-Enhanced Capture of Photons Using Optical Ratchet States

K. D. B. Higgins,[†] B. W. Lovett,[*,‡,†] and E. M. Gauger[*,§]

[†]Department of Materials, Oxford University, Oxford OX1 3PH, United Kingdom

[‡]SUPA, School of Physics and Astronomy, University of St Andrews, KY16 9SS, St Andrews, United Kingdom

[§]SUPA, Institute of Photonics and Quantum Sciences, Heriot-Watt University, EH14 4AS Edinburgh, United Kingdom

Supporting Information

ABSTRACT: Natural and artificial light harvesting systems often operate in a regime where the flux of photons is relatively low. Besides absorbing as many photons as possible, it is paramount to prevent excitons from annihilation via photon re-emission until they have undergone an irreversible energy conversion process. Taking inspiration from photosynthetic antenna structures, we here consider ringlike systems and introduce a class of states we call ratchets: excited states capable of absorbing but not emitting light. This allows our antennae to absorb further photons while retaining the excitations from those that have already been captured. Simulations for a ring of four sites reveal a peak power enhancement by up to a factor of 35 owing to a combination of ratcheting and the prevention of emission through dark-state population. In the slow extraction limit, the achievable power enhancement due to ratcheting alone exceeds 20%.

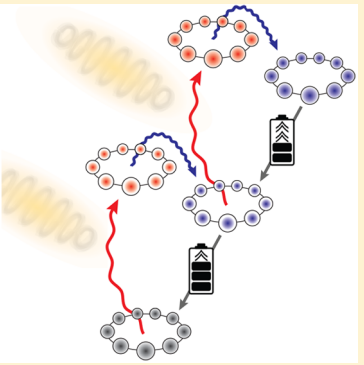

INTRODUCTION

The absorption of light and prevention of its reemission is essential for the efficient operation of solar energy harvesting devices.[1] From the many causes of device inefficiency, few are as fundamental and seemingly insurmountable as energy loss via radiative recombination: any absorption process must have a companion emission process. This inherent absorption inefficiency is a result of the principle of "detailed balance" and constitutes a key contribution to the famous Shockley–Queisser limit.[2] However, pioneering work by Scully showed that it is possible to break detailed balance, given an external source of coherence;[3] later work showed that this can be achieved by clever internal design alone, by using an optically dark state to prevent exciton recombination.[4−7] Such dark states are populated passively if the energy separation between dark and bright states falls into the vibrational spectrum of the absorbing nanostructure: dissipation then preferentially mediates transfer into states from which optical decay cannot occur. This is thought to play a role in photosynthetic light harvesters,[8,9] for example, by means of dynamic localization reducing the effective optical dipole strength.[10]

However, time spent in dark states is "dead time" with respect to absorbing further photons, which in models considered so far[4,7] would result in the loss of any subsequently arriving photons. In this article, we show that certain exciton states, which we will call ratchets, can enhance photocell efficiency by enabling absorption of these subsequent photons while preventing emission.

MODEL

We consider a ring of N identical two-level optical emitters (see Figure 1), with nearest pairs coupled by a transition dipole–dipole interaction,[11] governed by the Hamiltonian ($\hbar = 1$):

$$H_s = \omega \sum_{i=1}^{N} \sigma_i^+ \sigma_i^- + S \sum_{i=1}^{N} (\sigma_i^+ \sigma_{i+1}^- + \sigma_{i+1}^+ \sigma_i^-) \tag{1}$$

where ω is the bare transition energy of the sites, S is the hopping strength, the $\sigma_i^{\pm}$ denote the usual raising and lowering operators which create and destroy an excitation on site i, and $\sigma_{N+1} = \sigma_1$. In the case of a single exciton on the ring, each of the eigenstates is an equal superposition of localized excitations at the different ring positions, each characterized by a relative phase $k_j = 2\pi j/N$ with $j \in 0, 1, ..., N - 1$ between itself and adjacent positions. Higher excited states can be found using the Jordan–Wigner and Fourier transforms[12,13] and consist of multiple excitons, each with a distinct phase k_j. States with n excitons then form a band of eigenstates, each characterized by a set K of n different phase elements selected from the available k_j. If we label each eigenstate by its set of phases $|K\rangle$, with corresponding eigenvalue λ_K, then the Hamiltonian becomes $H_s = \sum_K \lambda_K |K\rangle \langle K|$ [see Supporting Information (SI)].

Optical transitions connect eigenstates differing by one exciton with rates proportional to $\Gamma_{K,K'} = |\langle K'|J^+|K\rangle|^2$ where $J^{\pm} = \sum_{i=1}^{N} \sigma_i^{\pm}$. An explicit analytical expression for $\Gamma_{K,K'}$ can be derived[13,14] and is given in the SI. Only the fully symmetric $k_j = 0$ single exciton eigenstate has a dipole matrix element with the ground state, since here the transition dipoles interfere constructively. The other $N - 1$ single exciton eigenstates do not couple to the ground state via light with a wavelength that is

Received: July 26, 2017
Revised: August 22, 2017
Published: August 23, 2017

DOI: 10.1021/acs.jpcc.7b07138
J. Phys. Chem. C 2017, 121, 20714−20719

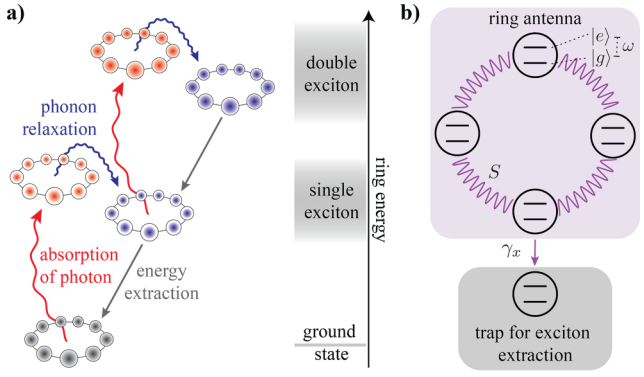

Figure 1. (a) Ratcheting cycle: (1) a photon is absorbed, moving the ring system from the ground state into the single excitation subspace; (2) phonon relaxation occurs into a state of the ring that is dark with respect to emission but which can absorb light; (3) a second photon may take the system up to the second excitation subspace; (4) once again, this is followed by rapid phonon relaxation. Extraction of energy is possible from both excited states. (b) Schematic of an $N = 4$ ring structure shown with intersite interactions and an attached trap system.

much longer than the separation between sites. However, these $N - 1$ states do have dipole-allowed transitions to the second exciton band. They, therefore, have the potential for preventing re-emission of light, while still allowing further absorption of photons, creating more excitons that in a photovoltaic circuit can be converted into useful photocurrent. Such states are examples of ratchet states $|K_R\rangle$, which have the simultaneous properties:

$$\Gamma^{-}_{K_R} := \sum_{K'} \Gamma_{K_R,K'} \delta_{|K_R|,|K'|+1} = 0 \tag{2}$$

$$\Gamma^{+}_{K_R} := \sum_{K'} \Gamma_{K_R,K'} \delta_{|K_R|,|K'|-1} > 0 \tag{3}$$

where $\Gamma^{-(+)}_{K_R}$ is the sum of all transition rates connecting the ratchet eigenstate $|K_R\rangle$ to the adjacent band below (above) and $\delta_{i,j}$ is the Kronecker symbol.

For $N = 4$ and $S > 0$, the bright state in the single exciton band has the highest energy $\omega + 2S$, and the three ratchet states have energies ω, ω and $\omega - 2S$, see Figure 2 and the SI. In a molecular system, the ratchet states can be reached following excitation into the bright state when the exciton loses a small amount of energy to molecular phonons (see Figures 1a and 2a). Importantly, such vibrational modes have much shorter wavelengths than optical modes and can often be assumed to be local to each site. Unlike the photon field, the phonon interaction then breaks the symmetry and enables intraband transitions.

DYNAMICS

To model the dynamics, we use the QuTiP package[15] to construct full open system dynamics in Bloch–Redfield theory, for each kind of environmental interaction. We always retain the full form of the resulting dissipator tensor since the secular approximation cannot be applied when a system has bands of closely spaced levels which may be more closely spaced than the corresponding dissipation rates.[16,17]

First, consider the dynamics due to the light-matter interaction Hamiltonian

$$H_{s-l} = \sum_{\mathbf{Q}} \sum_{i=1}^{N} G_{\mathbf{Q}} (\sigma_i^{+} b_{\mathbf{Q}} + \sigma_i^{-} b_{\mathbf{Q}}^{\dagger}) \tag{4}$$

where $b_{\mathbf{Q}}^{\dagger}$ and $b_{\mathbf{Q}}$ are creation and annihilation operators for photons of wavevector $\mathbf{Q}$. The photon spectral density is constant across all transition energies and enters into the master equation dissipator only via the single emitter decay rate γ_o. Absorption and stimulated emission terms are weighted by the appropriate Bose–Einstein factor $N(\omega_\Omega, T_o) = 1/(\exp[\omega_\Omega/(k_B T_o)] - 1)$, representing the thermal occupancy of the optical mode with interband transition frequency ω_Ω and at temperature T_o (5800 K for solar radiation). Our choice here assumes that the absorber is in radiative equilibrium with a blackbody emitter at the temperature of the sun. This can be achieved, for example, by suitable concentration of the sun's radiation, for example, by placing the absorber in a spherical cavity[18] (see also the discussion in the SI).

Second, the exciton–phonon interaction is accounted for through[19]

$$H_{s-p} = \sum_{i=1}^{N} \sum_{\mathbf{q}} g_{\mathbf{q},i} \sigma_i^{z} (a_{\mathbf{q},i} + a_{\mathbf{q},i}^{\dagger}) \tag{5}$$

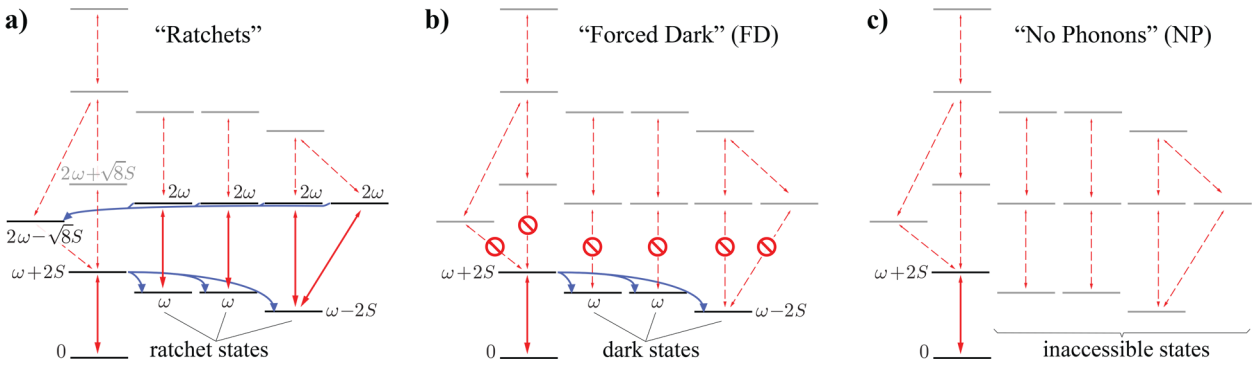

Figure 2. Transition process map and energy-level diagram of the three-ring antenna models studied in this paper. Solid red lines denote primary absorption transitions for each case of the light-harvesting cycle, whereas all other dipole-allowed optical transitions are depicted as thinner dashed red lines. The double arrowheads of these lines reflect the fact that absorption is invariably accompanied by a faster emission process. For clarity, only the most relevant phonon transitions are shown as solid blue arrows; their single arrowhead reflects the directional preference of phonon-induced relaxation. Rarely populated levels are shown in gray, whereas all black levels and solid optical/phonon transitions are important and feature in their respective cycle. The panels show (a) ratcheting, which is the natural configuration for an interacting ring antenna in condensed matter; (b) forced dark, where we artificially suppress optical transitions connecting the single and double excitation subspaces; (c) the ring antenna with all optical transitions allowed but in the absence vibrational relaxation.

DOI: 10.1021/acs.jpcc.7b07138
J. Phys. Chem. C 2017, 121, 20714–20719

where for each site i a_q and $a_q^\dagger$ are the creation and annihilation operators for phonons of wavevector $\mathbf{q}$ with energy ω_q and exciton−phonon coupling g_q. This interaction commutes with $\sum_i \sigma_i^z$ and so only mediates transitions within each excited band. For simplicity, we again assume a spectral density $J(\omega)$ that is approximately constant across all intraband transition energies ω_Π, such that $J(\omega_\Pi) = \gamma_p$. We calculate appropriate phonon matrix elements for each transition, letting absorption and stimulated emission terms carry the appropriate Bose−Einstein factors $N(\omega_\Pi, T_p)$, with T_p the ambient phonon temperature. Reflecting the fact that phonon relaxation typically proceeds orders of magnitude faster than optical transition rates,[20] we fix $\gamma_p = 1000\gamma_o$. This separation of time scales allows population to leave the bright states before reemission occurs.

To complete the photovoltaic circuit, we include an additional "trap site" t, with excited-state $|\alpha\rangle$ and ground-state $|\beta\rangle$, where excitons are irreversibly converted into work. The trap Hamiltonian is $H_t = \omega_t \sigma_t^+ \sigma_t^-$, where ω_t represents its transition frequency, and $\sigma_t^- = |\beta\rangle\langle\alpha|$. Henceforth, we shall consider the joint density matrix of the ring system and trap, $\rho = \rho_s \otimes \rho_t$. Throughout the paper, we use an incoherent hopping from a single site in the ring to the trap (see SI for an alternative model), and we fix the trap energy to be resonant with the state in which population is most likely to accumulate unless otherwise stated; this is at the bottom of the first exciton band, $\omega_t = \omega - 2S$.

The theory of quantum heat engines[4,21,22] provides a way for us to assess the current and voltage output of the ring device: The action of a load across the device is mimicked by the trap decay rate γ_t, which varies depending on the load resistance. The current is simply $I = e\gamma_t \langle\rho_\alpha\rangle_{ss}$, with $\langle\rho_\alpha\rangle_{ss}$ the steady-state population of the excited trap state. The potential difference seen by the load is given by the deviation of the trap's population from its thermal distribution:[4,22]

$$\mathrm{eV} = \hbar\omega_t + k_B T_p \ln\left(\frac{\langle\rho_\alpha\rangle_{ss}}{\langle\rho_\beta\rangle_{ss}}\right) \tag{6}$$

where k_B is Boltzmann's constant and T_p is the (ambient) phonon bath temperature. To study the relationship between current, voltage, and therefore power, we alter the trapping rate γ_t. Letting $\gamma_t \to 0$ or ∞ leads to the well-known open- and short-circuit limit, respectively; however, our main interest in the following is in the region near the optimal power output point of the device.

RESULTS AND DISCUSSION

We proceed by finding the steady state of the following master equation which incorporates the optical and phononic dissipator as well as the trap decay process:

$$\begin{aligned}\dot{\rho} = \; & -i[H_s + H_t, \rho] + D_o[\rho] \\ & + D_p[\rho] + D_t[\rho] + D_x[\rho]\end{aligned} \tag{7}$$

where $D_o[\rho]$, $D_p[\rho]$ are the Bloch−Redfield dissipators for the photon and phonon fields discussed earlier, and $D_t[\rho] = \gamma_t\left(\sigma_t^-\rho\sigma_t^+ - \frac{1}{2}\{\sigma_t^+\sigma_t^-, \rho\}\right)$ is a standard Lindblad dissipator representing trap decay. $D_x[\rho]$ represents exciton extraction via incoherent hopping at rate γ_x from a single site on the ring to the trap (see Figure 1b).

To expose the effect of the optical ratchets, we now contrast the full model of eq 7 with two other artificial cases that exclude the possibility of ratchets: In the first, the ratchet states are rendered fully dark by setting all upward transition matrix elements from them to zero, a scenario we refer to as "forced dark" (FD) as indicated in Figure 2b. In the second construct, we remove all phonon-assisted relaxation ($\gamma_p = 0$), meaning the system only undergoes optical transitions along the Dicke ladder of bright states;[17] we term this "no phonons" (NP), see Figure 2c. All results in this section are based on the steady state of the system for $N = 4$, obtained by an iterative numerical method performed with QuTiP[15] and using the default parameters from Table 1 unless explicitly stated otherwise. Our choice of $\omega = 1.8\ \mathrm{eV} - 2S$ differs from that in previous works:[4,5] our subtraction of $2S$ ensures that the highest (bright state) level in the first band always remains at 1.8 eV and absorbs at a fixed frequency.

Table 1. Default Model Parameters[a]

parameter	symbol	default value
atomic transition frequency	ω	$1.8\ \mathrm{eV} - 2S$
hopping strength	S	0.02 eV
spontaneous emission rate	γ_o	1.52×10^9 Hz $\equiv 1\ \mu$eV
phonon relaxation rate	γ_p	$10^3\ \gamma_o$
extraction rate	γ_x	$10^{-1}\ \gamma_o$
photon bath temperature	T_o	5800 K
phonon bath temperature	T_p	300 K

[a]Italic rows are plot parameters in certain figures, as stated in the relevant captions.

In Figure 3, we display the steady-state exciton population of the system without trapping as a function of optical and phonon bath temperatures. We compare the ratchet model to FD, finding that the ratchet enhancement is greatest in the hot photons, cold phonons regime. This is to be expected: hot photons quickly promote the system up the excited bands via ratchets, with cold phonons allowing a one-way protection of gained excitation energy. For FD states at low phonon temperature, the exciton population plateaus near one, as most of the population ends up trapped in the state at the bottom of the first band (see SI for the FD data and an extended discussion). By contrast, the ratchet states keep absorbing, allowing the steady-state population to rise toward the infinite temperature limit of 2 (for $N = 4$).

Using the heat engine model, we can now explore the performance of the four-site ring as an energy harvester. We will focus on the dependence of the power output on two parameters: the coupling S and the extraction rate γ_x. For each parameter set, the trap decay rate γ_t is varied for maximum power output; example power traces as a function of γ_t can be found the SI.

In Figure 4, we display the absolute value of the power generated for the ratchet and NP scenarios, whereas in Figure 5 we display the relative power output of ratchet states over each of the two artificial scenarios. To ensure fair comparison, for NP, we set the trap energy to be resonant with the bright state at $\omega + 2S$, since the ratchet states at lower energy are inaccessible here (cf. Figure 2c). All three scenarios have lower output power when the trapping (charge separation) rates are low, since this creates a bottleneck in the cycle and limits the size of the photocurrent.

However, the ratchet states hold a great advantage over the other scenarios in this bottlenecked region, since this is precisely the situation in which excitations need to be held for some time by the ring before extraction is possible. The NP scenario performs poorly in this case, since excitations in all likelihood decay before being extracted. Indeed, the relative power output of ratcheting over NP, shown in the left panel of Figure 5,

DOI: 10.1021/acs.jpcc.7b07138
J. Phys. Chem. C 2017, 121, 20714−20719

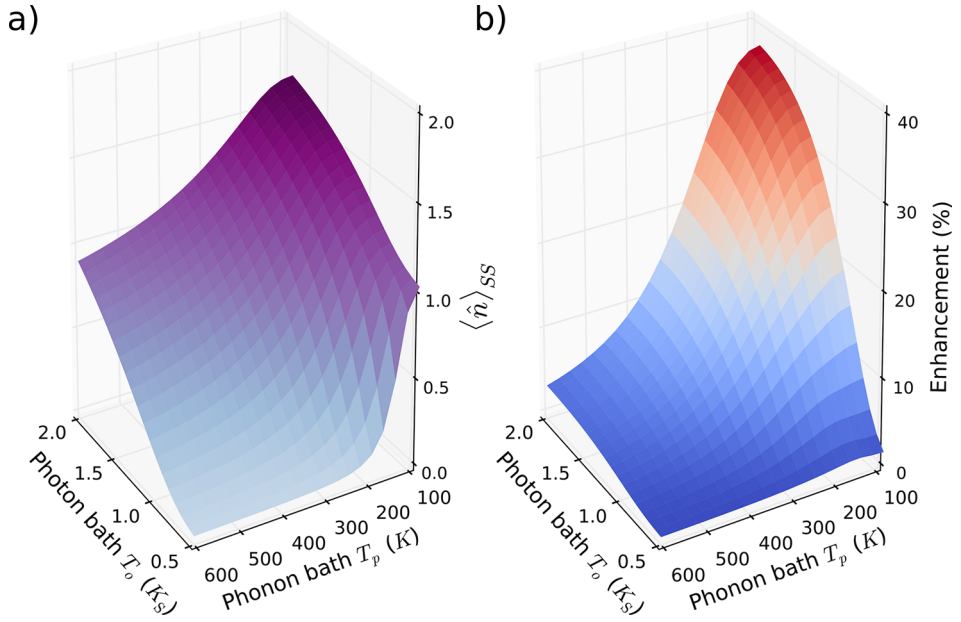

Figure 3. (a) Steady-state exciton population and (b) relative ratchet enhancement compared to the FD scenario (see text), both as functions of the optical and phononic bath temperatures and without any trap. The former is given in solar temperature units, K_S = 5800 K; other parameters are as in Table 1 except that $\gamma_x = 0$.

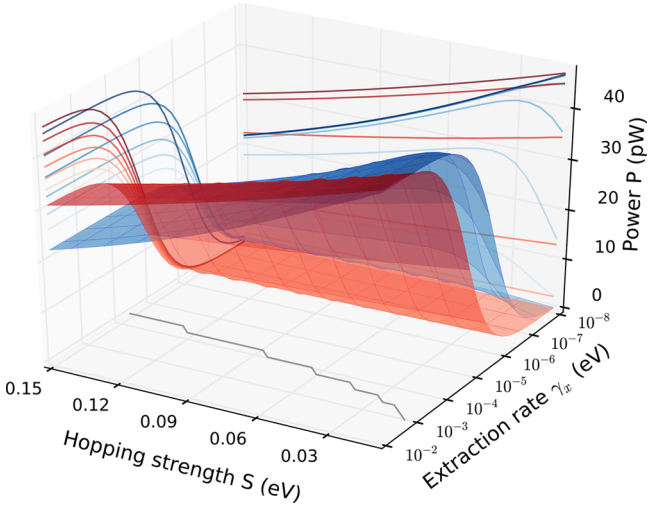

Figure 4. Absolute power output in the ratcheting (blue surface) and NP (red surface) cases as a function of (single site) extraction rate γ_x and hopping strength S. Other parameters are as in Table 1. For each point, the optimal trap decay rate is found by numerical search. The sets of curves projected onto the side walls of the 3D plot are cuts through the data for fixed values of the appropriate parameter. The two surfaces cross in the region where the bottleneck is lifted, with ratcheting generating more power for a severe and intermediate bottleneck. The line at which the curves cross is projected onto the bottom (xy) plane of the figure.

therefore rises to as high as a factor of 35. The right panel of Figure 5 demonstrates the importance of ratcheting over dark state protection alone, with the ratchet model delivering up to 20% better performance than FD. As previously discussed, this ratcheting enhancement over the dark-state protection relies on the absorber being in radiative equilibrium with the sun. By contrast, for a bare molecular ring antenna under direct solar illumination, the effective absorption rate is estimated to be several orders of magnitude lower (see SI). This renders the probability of ratcheting so low so as to no longer yield an appreciable advantage. Nevertheless, the dark-state protection mechanism remains operational and advantageous (cf. the left panel of Figure 5) in this scenario.

In Figure 5, we can see that the combined advantage of ratcheting and dark-state protection persists into a region where there is only a moderate bottleneck, that is, up to $\gamma_x \sim 10^{-5}$ eV = 10 γ_o. Referring to Figure 4, we see that the ratchet power output in this region is already close to its maximum. Even so, if the extraction rate was arbitrarily tunable, then even a moderate bottleneck could be avoided completely and the main advantage of ratcheting and dark-state protection could be removed. However, in photosynthesis, creating a fast extraction rate carries with it a clear resource cost: whereas antenna systems can be comparatively "cheap", reaction centers carry a much larger spatial footprint, being typically embedded in membranes and requiring significant surrounding infrastructure (such as concentration gradients produced by proton pumps). The severity of the bottleneck is likely to be inversely proportional to the number of reaction centers. A photocell design exploiting ratcheting in the moderate bottleneck regime would be likely then to generate optimal power per unit volume of material, and similar design principles will apply to artificially designed molecular light harvesting systems (see SI for a quantitative discussion).

The choice of interaction strength S is also important. Ratcheting achieves optimal results for $S \sim 0.05$ eV in the bottlenecked region. This dependence arises because the size of S determines the gap between bright and dark or ratchet states. In turn, this controls the effective rate for "upward" phonon-assisted transitions within excitation bands, as those rely on the absorption of a phonon and are proportional to $N(\omega_\Pi, T_p)$. Consequently, larger values of S entail more directed dissipation into the lower states of each band, boosting the occupation of ratchet states. However, at the same time, increasing S leads to a lower ratchet state energy and so a lower trap energy and, hence, to a voltage drop. The trade-off between these two competing influences leads to a maximum in ratchet performance.

The fill factor $P_{max}/(V_{max} \times I_{max})$, where P_{max} is the maximum power point and V_{max} and I_{max} are the open- and short-circuit

DOI: 10.1021/acs.jpcc.7b07138
J. Phys. Chem. C 2017, 121, 20714−20719

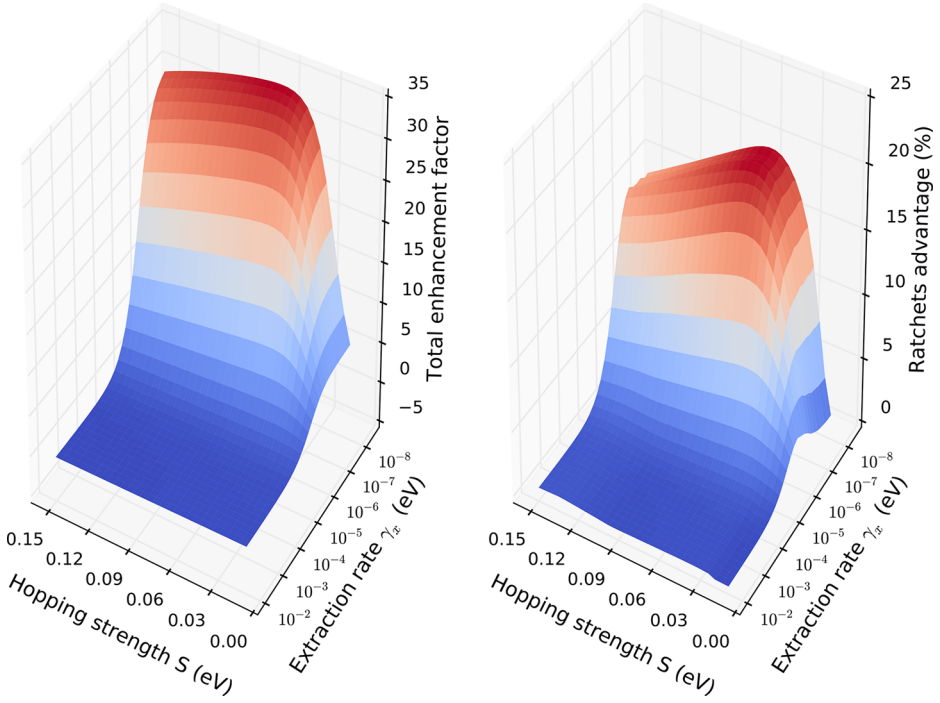

Figure 5. Enhancement of power output for ratchet states over NP (left, displayed as a multiplicative factor) and FD (right, displayed as a percentage), as a function of both hopping strength S and extraction rate γ_x. Parameters are as in Figure 4.

voltage and current, respectively, is an important indicator of the practical performance of photovoltaic devices. We plot fill factors obtained for our models in Figure S7 of the SI; these are all in the range $\approx 75 \pm 5$. Ratcheting scores consistently slightly below NP, however, the difference between the two remains small in the regime of interest, and ratcheting remains advantageous with an overall power output that is substantially higher than NP.

As we discuss in detail in the SI, ratcheting continues to convey an advantage in the presence of moderate levels of various real-world imperfections, such as site-energy disorder, nonradiative recombination, and exciton−exciton annihilation. In particular, we find that for modest disorder, that is, when the variation in site energies is less than the coupling strength, the performance of the ratchet model is broadly unaffected. Notwithstanding the fact that all our numerical results derive from a ring with $N = 4$, the single ratcheting step we have focused on is available for any ring size with $N \geq 3$. We note that a second tier of ratcheting requires $N \geq 5$; however, while ratcheting across multiple tiers may be of fundamental interest, we expect it to yield diminishing returns when it comes to boosting the output power of a photocell under the illumination condition considered in this study. As a consequence, there seems to be neither much of an advantage nor a fundamental drawback associated with moving to rings comprising more than four sites.

CONCLUSION

We have investigated the light-harvesting properties of coupled ring structures, inspired by the molecular rings that serve as antennae in photosynthesis. Considering a vibrational as well as an electromagnetic environment allows the system to explore the full Hilbert space rather than just the restricted subset of Dicke ladder states. We have shown that the off-ladder states possess interesting and desirable properties, which can be harnessed for enhancing both the current and the power of a ring-based photocell device. Dark-state protection is available under ambient conditions (i.e., direct sunlight illumination), whereas optical ratcheting unlocks additional advantages for systems brought into radiative equilibrium with the sun.

Several possible systems could be used to observe the effect (also see SI). These range from tailor-made demonstrator structures comprising superconducting qubits,[23] where the radiation field is in the microwave range. Closer in spirit to what we have proposed are macrocyclic molecules[24] with optical transitions, or NV[25] and SiV[26] centers in diamond, which have optical transitions that enable the study of the electronic dynamics at the single center level. Our approach generalizes existing concepts for dark-state protection[4,5] to arbitrary numbers of sites and importantly includes multiexciton states, which introduce the ratcheting effect as a distinct additional mechanism for enhancing the overall light-harvesting performance. The optical ratchet enhancement is particularly well suited to situations where exciton extraction and conversion represent the bottleneck of a photocell cycle.

In future work, it would be interesting to explore combining optical ratcheting with enhancements of the primary absorption process, for example, by exploiting the phenomena of stimulated absorption[27] or superabsorption.[17]

ASSOCIATED CONTENT

Supporting Information

The Supporting Information is available free of charge on the ACS Publications website at DOI: 10.1021/acs.jpcc.7b07138.

Diagonalization of coupled ring structures; explicit expressions for optical transition matrix elements; discussion of optical excitation rates; number of excitons in the steady state in the absence of extraction for all three scenarios discussed in the main text; an alternative extraction model; an example current and power vs voltage curve; calculated fill factor for all three models; snapshots illustrating the extraction bottleneck and hopping strength dependence;

DOI: 10.1021/acs.jpcc.7b07138
J. Phys. Chem. C 2017, 121, 20714−20719

maximizing higher power generation per unit area; a detailed discussion of imperfections (site-energy disorder, nonradiative recombination, and exciton−exciton annihilation); discussion of several systems that could be used to observe the effect
(PDF)

AUTHOR INFORMATION

Corresponding Authors

*E-mail: bwl4@st-andrews.ac.uk.
*E-mail: e.gauger@hw.ac.uk.

ORCID

E. M. Gauger: 0000-0003-1232-9885

Notes

The authors declare no competing financial interest.

ACKNOWLEDGMENTS

The authors thank William M. Brown for insightful discussions. This work was supported by the EPSRC and the Leverhulme Trust. B. W. L. thanks the Royal Society for a University Research Fellowship. E. M. G. acknowledges support from the Royal Society of Edinburgh and the Scottish Government. The research data supporting this publication are available online at http://dx.doi.org/10.17630/338044da-62e2-4582-a07f-2c42c304e869.

REFERENCES

(1) Kippelen, B.; Bredas, J.-L. Organic photovoltaics. *Energy Environ. Sci.* **2009**, *2*, 251−261.
(2) Shockley, W.; Queisser, H. J. Detailed Balance Limit of Efficiency of pân Junction Solar Cells. *J. Appl. Phys.* **1961**, *32*, 510−519.
(3) Scully, M. O. Quantum Photocell: Using Quantum Coherence to Reduce Radiative Recombination and Increase Efficiency. *Phys. Rev. Lett.* **2010**, *104*, 207701.
(4) Creatore, C.; Parker, M. A.; Emmott, S.; Chin, A. W. Efficient Biologically Inspired Photocell Enhanced by Delocalized Quantum States. *Phys. Rev. Lett.* **2013**, *111*, 253601.
(5) Zhang, Y.; Oh, S.; Alharbi, F. H.; Engel, G. S.; Kais, S. Delocalized quantum states enhance photocell efficiency. *Phys. Chem. Chem. Phys.* **2015**, *17*, 5743−5750.
(6) Yamada, Y.; Yamaji, Y.; Imada, M. Exciton Lifetime Paradoxically Enhanced by Dissipation and Decoherence: Toward Efficient Energy Conversion of a Solar Cell. *Phys. Rev. Lett.* **2015**, *115*, 197701.
(7) Fruchtman, A.; Gómez-Bombarelli, R.; Lovett, B. W.; Gauger, E. M. Photocell Optimization Using Dark State Protection. *Phys. Rev. Lett.* **2016**, *117*, 203603.
(8) Mukai, K.; Abe, S.; Sumi, H. Theory of Rapid Excitation-Energy Transfer from B800 to Optically-Forbidden Exciton States of B850 in the Antenna System LH2 of Photosynthetic Purple Bacteria. *J. Phys. Chem. B* **1999**, *103*, 6096−6102.
(9) Pearlstein, R. M.; Zuber, H. In *Antennas and Reaction Centers of Photosynthetic Bacteria: Structure, Interactions and Dynamics*; Michel-Beyerle, M. E., Ed.; Springer: Berlin, 1985; pp 53−61.
(10) Fidler, A. F.; Singh, V. P.; Long, P. D.; Dahlberg, P. D.; Engel, G. S. Dynamic localization of electronic excitation in photosynthetic complexes revealed with chiral two-dimensional spectroscopy. 2014, 5, 3286 EP. *Nat. Commun.* **2014**, *5*, No. 10.1038/ncomms4286, DOI: 10.1038/ncomms4286.
(11) Note that we here assume all optical dipoles are aligned perpendicular to the plane of the ring, which is different from the tangential alignment typically encountered in photosynthetic rings.
(12) Jordan, P.; Wigner, E. Über das Paulische Äquivalenzverbot. *Zeitschrift für Physik* **1928**, *47*, 631−651.
(13) Tokihiro, T.; Manabe, Y.; Hanamura, E. Superradiance of Frenkel excitons in linear systems. *Phys. Rev. B: Condens. Matter Mater. Phys.* **1993**, *47*, 2019−2030.
(14) Spano, F. C. Fermion excited states in one-dimensional molecular aggregates with site disorder: Nonlinear optical response. *Phys. Rev. Lett.* **1991**, *67*, 3424−3427.
(15) Johansson, J.; Nation, P.; Nori, F. QuTiP 2: A Python framework for the dynamics of open quantum systems. *Comput. Phys. Commun.* **2013**, *184*, 1234−1240.
(16) Eastham, P. R.; Kirton, P.; Cammack, H. M.; Lovett, B. W.; Keeling, J. Bath-induced coherence and the secular approximation. *Phys. Rev. A: At., Mol., Opt. Phys.* **2016**, *94*, 012110.
(17) Higgins, K. D. B.; Benjamin, S. C.; Stace, T. M.; Milburn, G. J.; Lovett, B. W.; Gauger, E. M. Superabsorption of light via quantum engineering. *Nat. Commun.* **2014**, *5*, 4705.
(18) Würfel, P.; Würfel, U. *Physics of Solar Cells: From Basic Principles to Advanced Concepts*, 3rd ed.; Wiley-VCH: Weinheim, 2016.
(19) Mahan, G. D. *Many Particle Physics (Physics of Solids and Liquids)*, 3rd ed.; Springer: New York, 2000.
(20) Brinks, D.; Hildner, R.; van Dijk, E. M. H. P.; Stefani, F. D.; Nieder, J. B.; Hernando, J.; van Hulst, N. F. Ultrafast dynamics of single molecules. *Chem. Soc. Rev.* **2014**, *43*, 2476−2491.
(21) Scully, M. O.; Chapin, K. R.; Dorfman, K. E.; Kim, M. B.; Svidzinsky, A. Quantum heat engine power can be increased by noise-induced coherence. *Proc. Natl. Acad. Sci. U. S. A.* **2011**, *108*, 15097−15100.
(22) Dorfman, K. E.; Voronine, D. V.; Mukamel, S.; Scully, M. O. Photosynthetic reaction center as a quantum heat engine. *Proc. Natl. Acad. Sci. U. S. A.* **2013**, *110*, 2746.
(23) Mlynek, J. A.; Abdumalikov, A. A.; Eichler, C.; Wallraff, A. Observation of Dicke superradiance for two artificial atoms in a cavity with high decay rate. *Nat. Commun.* **2014**, *5*, 5186.
(24) O'Sullivan, M. C.; Sprafke, J. K.; Kondratuk, D. V.; Rinfray, C.; Claridge, T. D. W.; Saywell, A.; Blunt, M. O.; O'Shea, J. N.; Beton, P. H.; Malfois, M.; et al. Vernier templating and synthesis of a 12-porphyrin nano-ring. *Nature* **2011**, *469*, 72−75.
(25) Waldherr, G.; Wang, Y.; Zaiser, S.; Jamali, M.; Schulte-Herbruggen, T.; Abe, H.; Ohshima, T.; Isoya, J.; Du, J. F.; Neumann, P.; et al. Quantum error correction in a solid-state hybrid spin register. *Nature* **2014**, *506*, 204−207.
(26) Sipahigil, A.; Evans, R. E.; Sukachev, D. D.; Burek, M. J.; Borregaard, J.; Bhaskar, M. K.; Nguyen, C. T.; Pacheco, J. L.; Atikian, H. A.; Meuwly, C.; et al. An integrated diamond nanophotonics platform for quantum-optical networks. *Science* **2016**, *354*, 847−850.
(27) Kavokin, A.; Eramo, G. Photocurrents induced by stimulated absorption of light. *Nat. Sci.* **2010**, *2*, 63−66.

DOI: 10.1021/acs.jpcc.7b07138
J. Phys. Chem. C 2017, 121, 20714−20719